Ingeniería Investigación y Tecnología
Volume XXVI (Issue 4), October-December 2025 1-12
ISSN 2594-0732 FI-UNAM Peer-reviewed article
Article information: Received: February 11, 2025, accepted: June 24, 2025

https://doi.org/10.22201/fi.25940732e.2025.26.4.025

Ingeniería
Investigación y
Tecnología

Quantitative and objective full-field strain measurements of healthy human skin during distal upper extremity range of motion

López-Lugo, Jonathan David
Universidad Nacional Autónoma de México
Instituto de Investigaciones en Materiales
E-mail: jonathandlpzlgo@gmail.com
https://orcid.org/0000-0003-3095-967X

Benítez-Martínez, Jorge Alejandro
Universidad Nacional Autónoma de México
Instituto de Investigaciones en Materiales
E-mail: jbenitez1393@gmail.com
https://orcid.org/0000-0003-2316-6946

Alvarez-Camacho, Michelín (Corresponding autor)
Universidad Nacional Autónoma de México
Ingeniería en Sistemas Biomédicos
Instituto Nacional de Rehabilitación, Luis Guillermo Ibarra Ibarra
E-mail: mich_address@hotmail.com
https://orcid.org/0000-0003-1540-9522

Leyva-Gómez, Gerardo
Universidad Nacional Autónoma de México
Departamento de Farmacia
E-mail: leyva@quimica.unam.mx
https://orcid.org/0000-0002-7940-1100

Morales-García, Mariana
Instituto Nacional de Rehabilitación, Luis Guillermo Ibarra Ibarra
E-mail: Mogama79@gmail.com
https://orcid.org/0009-0004-7629-9130

Palacios-Morales, Carlos
Universidad Nacional Autónoma de México
Ingeniería en Sistemas Biomédicos
E-mail: cpalacios@unam.mx
https://orcid.org/0000-0001-9161-3205

Sánchez-Arévalo, Francisco Manuel
Universidad Nacional Autónoma de México
Instituto de Investigaciones en Materiales
E-mail: fsanchez@materiales.unam.mx
https://orcid.org/0000-0003-4369-1262

Abstract

Traditional tools for assessing burns, such as the Vancouver Scar Scale and Cutometry, provide only subjective or localized mechanical evaluations. These methods lack the capacity to deliver comprehensive, objective data on skin deformation, particularly during dynamic movement. This study aims to demonstrate the utility of 3D-Digital Image Correlation (3D-DIC) as a non-invasive, quantitative technique for capturing full-field strain and displacement responses of the skin throughout the complete articular range of motion of the distal upper extremity. An in vivo experimental protocol was applied to a healthy subject to evaluate the mechanical behavior of the skin on the dorsal hand and volar forearm. 3D-DIC was used to quantify strain and displacement during metacarpophalangeal flexion (MF), composite fist (CF), wrist flexion (WF), and wrist extension (WE). Cutometry was also applied on volar and dorsal regions of the forearm to obtain comparative strain profiles under localized suction. 3D-DIC revealed semicircular skin recruitment patterns. Maximum displacements of 9 mm and 11 mm were observed for MF and CF, respectively, with corresponding maximum strains of 30 % and 35 %. During WF and WE, displacements ranged from 10-12 mm, with the highest strain localized near the radiocarpal joint. While Cutometry and 3D-DIC yielded different strain behaviors, the two methods proved complementary, enhancing the understanding of skin deformation under different mechanical stimuli. These findings suggest that 3D-DIC can serve as a robust, objective tool for evaluating skin mechanics in clinical and research settings, especially for applications involving scar assessment, surgical planning, and rehabilitation monitoring.
Keywords: Cutometer, digital image correlation, mechanical behavior, skin deformation, skin displacement.

https://doi.org/10.22201/fi.25940732e.2025.26.4.025

Introduction

Chronic wounds, defined as those that fail to heal within approximately three months, are a growing global health challenge, with a prevalence of around 0.18 % – 0.32 % in the general population, and up to 2 % in developed nations (Järbrink *et al.,* 2016; Olsson *et al.,* 2018; Vázquez *et al.,* 2019; vanAlpen *et al.,* 2023). Burn injuries constitute a significant subset of chronic wounds. In high-income countries, 2 % – 6 % of burn wounds become chronic, but this rate rises dramatically -to 12 % – 41 %- in lower-resource settings (Frykberg & Banks, 2015). Hospital data also indicate that 10 % – 70 % of burn admissions involve the hand or wrist, and approximately 50 % of those affect both hands due to instinctive protective reflexes (Moore *et al.,* 2009).

Treating burns of the hand presents unique challenges, given the need to preserve mobility, sensation, and extensive joint range. Multidisciplinary burn units are critical to preventing functional loss (Maslauskas *et al.,* 2009). Particularly, contracture formation, pathological scar tissue shortening that restricts motion and alters anatomy, is one of the main complications of burns (Reginald, Rl *et al.,* 2009). Current treatments include permanent autografts or dermal matrices, and temporary xenografts/allografts (Elseth & Nunez, 2021). However, evaluating outcomes has traditionally relied on subjective, superficial tools (Fearmonti *et al.,* 2010), such as the Patient and Observer Scar Assessment Scale (Draaijers *et al.,* 2004) and the Vancouver Scar Scale d (Nedelec *et al.,* 2000; Sullivan *et al.,* 1990). The main advantage of these two scales lies in their ease of implementation, which has contributed to their widespread use around the world. However, both are inherently subjective and suffer from limited reproducibility. Therefore, there is a need for more consistent methodologies and objective measurement techniques using advanced instruments (Ud-Din & Bayat, 2016).

In recent years, there has been a substantial rise in clinical and preclinical studies exploring biomechanical monitoring of wound healing using techniques such as suction (Mueller *et al.,* 2021; Boyer *et al.,* 2011; Diridollou *et al.,* 2000; Barel *et al.,* 1998) indentation (Paillet-Mattei *et al*., 2008), tension (Delalleau *et al.,* 2008), torsion (Agache *et al.,* 1980) and double exposure photography (DEP) technique, used to determine displacement fields of human skin under normal range of motion (RoM) and to identify cutaneous functional (Richard *et al.,* 2009).

Indentation and torsion techniques are predominantly used in research environments rather than in routine clinical practice, as their output can vary significantly with experimental parameters. For instance, in vivo indentation of forearm skin has reported Young's moduli around 4.5-8 kPa, but precise values depend on probe size, indentation speed, tissue hydration, and anatomical site (Blair *et al.,* 2020; Pailler *et al.,* 2008). Torsion tests, applying controlled torque to measure viscoelastic response, yield moduli in the 0.4-1.1 MPa range, yet results are inconsistent unless factors like skin orientation and fixture method are standardized (Blair *et al.,* 2020). Critically, both techniques require replicating the complex state of stress and strain generated during natural movement, but they are typically conducted under static or constrained conditions that do not reflect in vivo biomechanics. As a result, achieving reliable, physiologically relevant measurements remains challenging.

Cutometry is a suction-based technique that is widely used in both clinical and research settings to assess the mechanical properties of skin (Mueller *et al.,* 2021). It offers high reproducibility, portability, and rapid, minimally invasive measurements (Held *et al.,* 2014). However, it is a point-based method, relying on probes typically ranging from 2 to 8 mm in diameter, which limits its applicability for evaluating larger anatomical regions. Additionally, there remains inherent uncertainty regarding the contribution of skin depth and underlying structures to the measured suction-strain response. To overcome these limitations and achieve a more comprehensive understanding of strain and stress distribution, complementary techniques are recommended. One such technique is Digital Image Correlation (DIC), a non-contact optical method capable of capturing full-field strain and displacement measurements under physiological motion. This is particularly relevant for analyzing complex, dynamic regions such as the hands and wrists. DIC provides spatially resolved visual maps of mechanical behavior with high accuracy and low error margins (Xu *et al.,* 2019), making it a powerful tool for biomechanical skin analysis in both research and clinical applications.

Digital Image Correlation (DIC) has been employed to evaluate the mechanical behavior of human skin in both in vitro and in vivo contexts. In early applications, Marcellier *et al.* (2001) conducted 2D in-plane strain measurements using DIC on excised human skin samples, combining the technique with extensometry and cutometry to enhance the accuracy and richness of mechanical data in vitro. Later, Evans & Holt (2009) applied DIC to measure skin displacement on the forearm in vivo under a 5 N transverse load. Their findings revealed a maximum displacement of approximately 8.5 mm, as well as local wrinkling near the application point, demonstrating the technique's sensi-

tivity to subtle mechanical responses. In 2014, Podowojewski *et al.* utilized DIC to characterize the biaxial mechanical behavior of the human abdominal wall ex vivo under inflation loading. Their study evaluated tissue deformation before and after surgical mesh implantation, revealing that the longitudinal strain (parallel to the linea alba) increased from 6.0 % at baseline (50 mmHg) to 7.9 % post-incision, and returned to 6.8 % following mesh repair. These examples underscore DIC's capacity to provide detailed, spatially resolved insights into tissue mechanics under clinically relevant conditions.

In 2015, Wilson *et al.* employed DIC to investigate the effects of botulinum toxin on facial dynamics. Their study demonstrated a marked reduction in skin deformation following neurotoxin injection: vertical stretch in the glabella decreased from 2.51 % to 1.15 %, and in the forehead from 6.73 % to 1.67 %. These findings highlighted the utility of DIC in evaluating facial kinematics, particularly in the context of aging and neuromuscular modulation. In another study, Khatam *et al.* (2014) combined stereophotogrammetry with DIC to assess changes in breast skin deformation during positional transitions from supine to upright. They reported a significant increase in the principal stretch ratio, from 1.25 to 1.60, particularly in the region above the nipple, illustrating how gravitational forces alter soft tissue mechanics. Similarly, Maiti *et al.* (2016) used DIC in conjunction with optical coherence tomography to analyze forearm skin deformation induced by joint movement. They reported strain values of ε_{xx} = 5.6 % along the medial forearm and ε_{yy} = 23.3 % along the proximal direction at full extension. The study reinforced DIC´s value as a robust, non-invasive tool for capturing the biomechanical response of skin under natural motion conditions.

In 2017, Xue *et al.* used 2D DIC to measure skin strain on the dorsal hand during finger extension, reporting a maximum strain of approximately 3.3 % at the metacarpophalangeal joint of the third finger. In 2018, Solav *et al.* applied 3D DIC to the calf region during ankle plantar flexion and observed a compressive stretch ratio around –1.1, suggesting its diagnostic value for early-stage treatment planning. More recently, Chen *et al.* (2020) introduced a panoramic DIC setup using mirrors to capture forearm skin deformation during fist clenching, reporting maximal principal strains of about 0.1 %, which demonstrated DIC's versatility for capturing fine mechanical responses.

Although numerous studies have explored the application of Digital Image Correlation (DIC) to assess the mechanical behavior of human skin, there remains a need for standardized, full-field evaluations of strain and displacement throughout the entire articular range of motion. Conventional assessment tools commonly used in burn management, such as the Vancouver Scar Scale and Cutometry, offer either subjective functional evaluations or localized mechanical measurements, respectively. However, these approaches are limited in their ability to capture the comprehensive mechanical and functional behavior of the skin. As such, there is a pressing need for methodologies that enable simultaneous, quantitative, and objective evaluation of both function and mechanical response. Therefore, the main objective of this study is to demonstrate that 3D-DIC is a suitable technique for capturing full-field strain and displacement measurements of the skin in the distal upper extremity throughout the full articular range of motion.

Furthermore, we specifically selected four common hand and wrist movements: Metacarpophalangeal flexion, composite fist, wrist extension, and wrist flexion, to examine the recruitment zones of skin across the upper limb surface, given that there is no clear evidence in the literature describing de patterns and regions of displacement and deformation to permit these joint motions. This gap is particularly relevant because these gestures are typically evaluated during the examination of burned hands in clinical settings.

Methodology: subjects and methods

Subjects

An *in vivo* study was performed to explore healthy forearm and dorsal hand skin. The strain profiles of the volar and dorsal forearm skin were obtained using a Cutometer. Deformation and strain for the complete RoM, for metacarpophalangeal flexion, composite fist, wrist flexion, and wrist extension, were also evaluated using 3D-DIC to compare their mechanical responses. Three men participated in the study. They aged between 23 and 24 years with a Body Mass Index (BMI) ranging 23-24.5. Volunteers were free of scars in the dominant arm and had no history of skin disease or orthopedic conditions affecting joint RoM. Each subject signed an informed consent form according to the WMA Declaration of Helsinki, and all research was approved by the Research Committee of Instituto Nacional de Rehabilitación Luis Guillermo Ibarra Ibarra, registration number 31/17. Subjects were asked to shave the forearm 48 hours before the experiment, avoid using cosmetics or moisturizers 24 hours before the test, and perform standard morning cleaning. The subjects were allowed to rest 50 minutes before data acquisition in a room without direct sun exposure. Data

acquisition for 3D-DIC and Cutometer were recorded a week apart to avoid the interaction of methods. Just the most representative case is presented in this work.

Methods

3D-Digital Image correlation

For data acquisition, we used the ARAMIS 5LMT, GOM system, and its processing software version 6.3 (GOM mbh, 2009). ARAMIS 5LMT consists of two adjustable stereo vision cameras with 5 MPixels of resolution (2448x2050 pixels), an external white light source, and a laser pointer. An area of interest was defined from the metacarpus to the elbow of the subjects. Thus, the resulting measuring volume was 330 x 250 x 120 mm in length, width, and height, respectively. Noticing that the center of the arm's surface -to be measured- matches the measuring volume's center, Figure 1a shows the 3D-DIC cameras setup. The distance between cameras was 254 mm and the distance to the volume center was 660 mm; additionally, a CP 20 350X280 calibration panel was used. After the calibration procedure according to ARAMIS 6.1 user Manual-Software, we obtained calibrated images exhibiting a pixel size of 0.16 mm and a permissible error < 0.04 pixel. In these measurements we defined the positive Y-axis point towards the proximal direction and the negative Y corresponds to the distal direction. In addition, a device was constructed to control the position of the upper extremity in the initial and final positions, to eliminate accessory movement during the test of metacarpophalangeal flexion, compound fist, wrist flexion, and wrist extension ROMs. Thus in the next subsection skin preparation details will be exposed.

Skin preparation

The 3D-DIC technique requires specific surface preparation to enhance the correlation process. For this study a preparation method was developed for external use only. The forearm of the subjects was coated with a thin layer of white artistic makeup, (Createx, México). We applied the makeup from the flexion crease of the elbow until the proximal interphalangeal joint for the dorsal region. Additionally, seven reference marks were drawn to facilitate the analysis: transverse crease over the radiocarpal joint, two inches proximal to the transverse crease over the radiocarpal joint, flexion crease of the elbow, the half distance between wrist crease and elbow crease, the middle line of hand, projection of the transverse palmar crease to the hand dorsum and 10 mm proximal to the transverse palmar crease. In the volar forearm, the makeup covered from

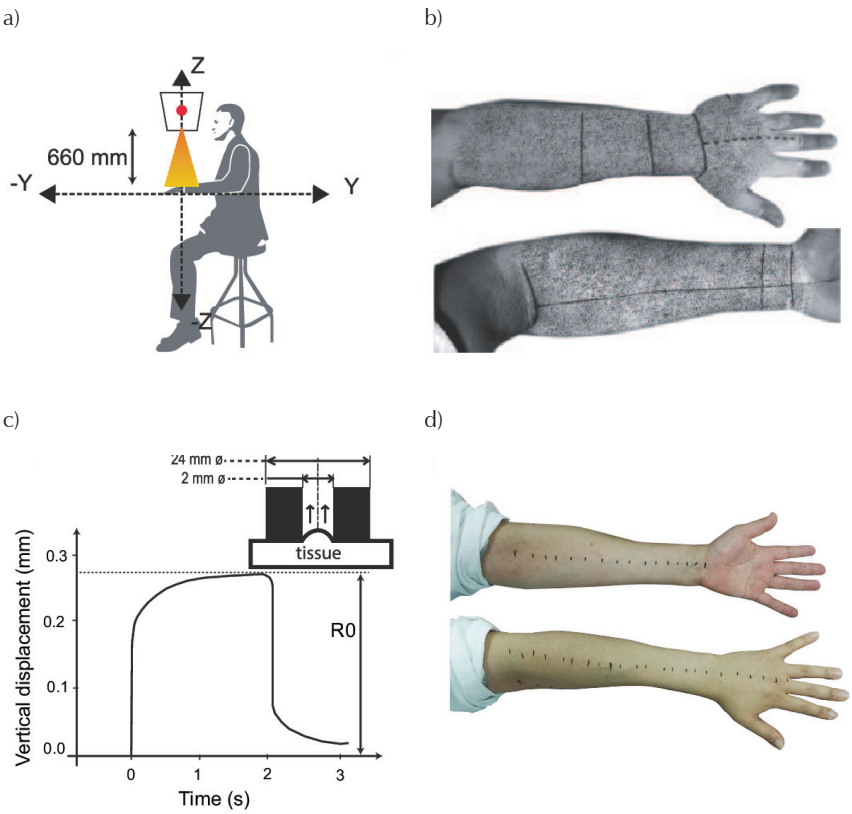

Figure 1. Cutometry and 3D-DIC experimental setups. a) DIC cameras setup, b) skin preparation and seven reference marks for DIC measurements, c) cutometer probe diagram. The coordinate axes of the measurement are shown. +Y proximal, -Y distal. d) Measured points on the arm with cutometer.

the flexion crease of the elbow to the distal transverse wrist crease and four reference marks were drawn: transverse wrist crease, flexion crease of the elbow, one inch proximal to the distal transverse wrist crease, and the longitudinal axis of the forearm. Figure 1b shows the skin preparation on the forearm and the reference marks.

Besides, a stochastic pattern of black points over the white background, was applied spreading black eye makeup powder; the quality of the preparation was checked before data collection, the measurement error was less than 0.04 pixels. Subjects were seated beside a table with their forearm supported on the custom positioning device for data acquisition.

Data acquisition

A sampling frequency of 10 Hz was used in all cases. Subjects performed four trials of the desired joint movement to familiarize themselves with the movement and to precondition the skin, prior to data acquisition. All movements were performed in an active manner, except for wrist extension to 70 degrees, which was conducted in an active-assisted fashion. Assistance was provided to ensure that full RoM occurred among the volunteers.

Measured joint movements

Metacarpophalangeal flexion (MF)

A measurement region was defined from the head of the metacarpals to the middle of the forearm. For the initial position, the hand was placed matching the reference mark of the projection of the transverse palmar crease to the hand dorsum with the edge of the table and positioning device, in pronation and full extension. The middle line of the hand was positioned perpendicular to the transverse crease over the radiocarpal joint, to obtain the neutral position. The subjects were asked to perform the metacarpophalangeal flexion movement, starting from the neutral position to the final position at 90 degrees and to return to neutral. The total acquisition time was 6 seconds.

Composite fist (CF)

A measuring region was defined from the head of the metacarpals to the middle of the forearm. In the initial position, the forearm was placed 10 mm proximal of the transverse palmar crease mark at the edge of the positioning device in full pronation. The middle line of the hand was perpendicular to the transverse crease over the radiocarpal joint. After this alignment, the subjects were asked to progressively perform the interphalangeal distal and metacarpophalangeal flexion movement, using only from the second to the fifth phalanx. The subject was asked to make the previously described movement in 4 seconds and return to the initial position in 4 seconds for data collection. Data were recorded for 12 seconds.

Wrist flexion (WF)

The measuring region was defined from the transverse distal wrist crease to the flexion creases of the elbow. For the initial position, the hand was placed with the fist closed, matching the mark 2 inches proximal to the wrist crease with the edge of the positioning device and the table, the midline of the hand perpendicular to the line of the crease of the wrist. For data collection, the subject was asked to perform the wrist flexion from the initial position to the final position at 90 degrees and back in 8 seconds. Data were recorded for 12 seconds.

Assisted wrist extension (WE)

A measurement region was defined from the transverse wrist crease to the flexion crease of the elbow. For the initial position, the arm was placed matching the mark 1 inch proximal to the wrist crease with the edge of the positioning device. The longitudinal axis of the forearm was perpendicular to the wrist crease. The subjects were assisted in extending the wrist to 70 degrees and returning to a neutral position in a controlled fashion. The complete movement took 8 seconds, and data were recorded for 12 seconds.

The full-field displacement and principal strain maps were calculated for the final position of four joint movements. Principal strains were reported and allow an absolute comparison of the strains measurement over the interest joints. A detailed analysis was performed along the longitudinal axes in five sequential positions for each movement.

Cutometry

To evaluate the strain response of the skin surface undergoing suction, a Cutometer 580, Courage + Khazaka electronic GmbH with a 2 mm internal diameter probe was used. Measuring sites were selected at the dorsal and ventral forearm. Measuring marks were placed on the longitudinal axis of the dorsal forearm from the flexion crease of the elbow to the proximal interphalangeal joint; and on the longitudinal axis of the volar forearm from the flexion crease of the elbow to the distal transverse wrist crease, at 1 cm distance as shown in Figure 1d.

Ten suction cycles of 450 mbar were applied, with a pattern of two seconds of suction and two seconds for skin relaxation, and a sampling frequency of 100 Hz.

The curves of the penetration height of the skin into the probe as a function of time were registered. Figure 1c shows a lateral view of the cutometer probe, and a typical curve obtained by Cutometry. R0 was found from the curve, as the maximum height registered in the first cycle of actuation.

The cutometer responses were contrasted with 3D-DIC skin mechanical response along the longitudinal axis of the hand dorsum and forearm. These measurements were conducted over the dorsal forearm provoked by metacarpophalangeal flexion; the strain in the volar forearm was generated by wrist extension. The strain data from DIC was processed as follows: an early stage from each of 3 different experiments were selected and averaged to obtain the maximum strain values. Then, to contrast the response these data were superimposed with the R0 parameter from the Cutometry.

Results

Full-field displacement and major strain maps of the forearm skin were obtained from the tested subjects through 3D- DIC during the joint movement when performing the full range of joint motion of MF, CF, WF and WE. The generated maps permitted the observation of the recruitment patterns generated over the tested joint and its vicinity.

The maps generated by metacarpophalangeal flexion (MF) and composite fist (CF) are shown in Figure 2. The obtained displacement maps made it possible to quantify the displacement generated by the full RoM of the metacar- pophalangeal joint and visualize the skin recruitment in each axis separately. For MF, in the x-axis (medial to lateral), a maximum displacement of – 2 mm was measured in the head of the fifth metacarpal; additionally, a displacement of +3 mm in the head of the second metacarpal was detected as shown in (Figure 2a). Here, the lateral ends of the hand dorsum presented a displacement with opposite direction respect to each other. While in the y-axis (proximal to distal), a semicircular recruitment pattern was formed in the dorsal hand, with a maximum displacement of –9 mm found in the head of the third metacarpal (Figure 2b). The displacement response for CF full RoM followed a similar pattern with a magnitude between – 4 mm and +8 mm in the heads of the fifth and second metacarpal respectively for the x-axis (Figure 2d), and – 11 mm in the head of the third metacarpal for the y-axis (Figure 2e). In the generated maps, it was possible to quantify the response of major strain and displacement data separately. For the metacarpophalangeal joint, the full field major strain pattern generated by MF and CF shows the maximum deformation; it was localized in the head of the metacarpals, with a magnitude of 30 % for MF (Figure 2c) and 35 % for CF (Figure 2f). Notice that the strain of the skin was located mainly at the hand dorsum; furthermore, we observed that for these two movements, the strain of the skin was essentially null at the forearm.

Quantitative displacement and major strain maps were obtained from the forearm skin of the test subjects for wrist flexion (WF) and wrist extension (WE) for the full RoM. These maps show that the maximum displacement occurred near the radiocarpal joint, in the proximal to distal direction, with maximum values of –10 mm for WF and –12 mm for WE (see Figures 3a and c). The major strain maps obtained for WF and WE full RoM (see Figures 3b and d) show that the maximum strain occurred near the radiocarpal joint. For the case of WF we also observe that the displacement field along the forearm presented values close to 4 mm (see Figure 3a); besides it was detected that the strain increased along the same region as shown in Figure 3b; these might be due to muscular volume change which is required during the articular motion.

A detailed analysis of skin displacement was performed also with 3D-DIC. This analysis was conducted in five arbitrary positions between the initial and final RoM. It allowed to quantify the recruitment of the skin in intermediate instants during RoM. This analysis was performed for the four joint movements of interest, along the midline of the volar and dorsal forearm Figure 4. Since the length of the analyzed surface changed during the increase in articular angle, we presented these results in percentages indicating relative positions on the forearm. In these four cases, the maximum displacement appears near the articular joints where the movement begins. Mainly, we detected the most important displacement during the full RoM, yielding values of 8 mm for MF, 10 mm for CF, 10 mm for WF, and beyond 12 mm for WE. For MF and CF, the displacement and recruitment of the skin is not carried out beyond 50 % of the measurement area, that is, only the surface of the back of the hand is involved and not the forearm. On the contrary, for WF and WE, recruitment is done in almost the entire area of the forearm. The displacement curves increased in a homogeneous fashion, except in the WF case, where the area of interest for the forearm exhibited greater displacement than in the other cases. This may be due to changes in the volume of underlying wrist flexors.

In addition to displacement, the skin in the upper arm extends to permit articular movement, 3D-DIC technique allowed the quantification of strain individually, to observe the skin extension capability. Figure 5 shows five sequential profiles indicating the major stra-

in along the longitudinal axis of the forearm for the four joint movements. Similarly, as in the displacement charts, we also located the maximum value of major strain near the metacarpal heads, 25 % for MF and 22 % for CF; major strain increased over the hand dorsum from the wrist up to the metacarpophalangeal heads for both movements. Besides, we observed a maximum value of major strain of 31 % near the radiocarpal joint for WF. Again, as in the displacement chart, two peaks of 10 % and 8 % were observed in the forearm. In the case of wrist extension, a 35 % of major strain was located at the radiocarpal joint.

The strain behaviors obtained with 3D-DIC and Cutometry were dissimilar, due to the different nature and procedures to measure strain in both methods. Figure 6 depicts strain data obtained with 3D-DIC along the longitudinal axis of the hand dorsum and forearm, compared with the R0 parameter from the Cutometer, obtained over the same region of interest. For both cases, the strain was normalized with the maximum value. Notice that the Cutometer gives a very punctual measurement based on the step response of the skin to an external applied force (suction pressure) perpendicular to the skin plane. On the other hand, the DIC technique measures the 3D displacements and strain on the skin surface provoked by articular movement.

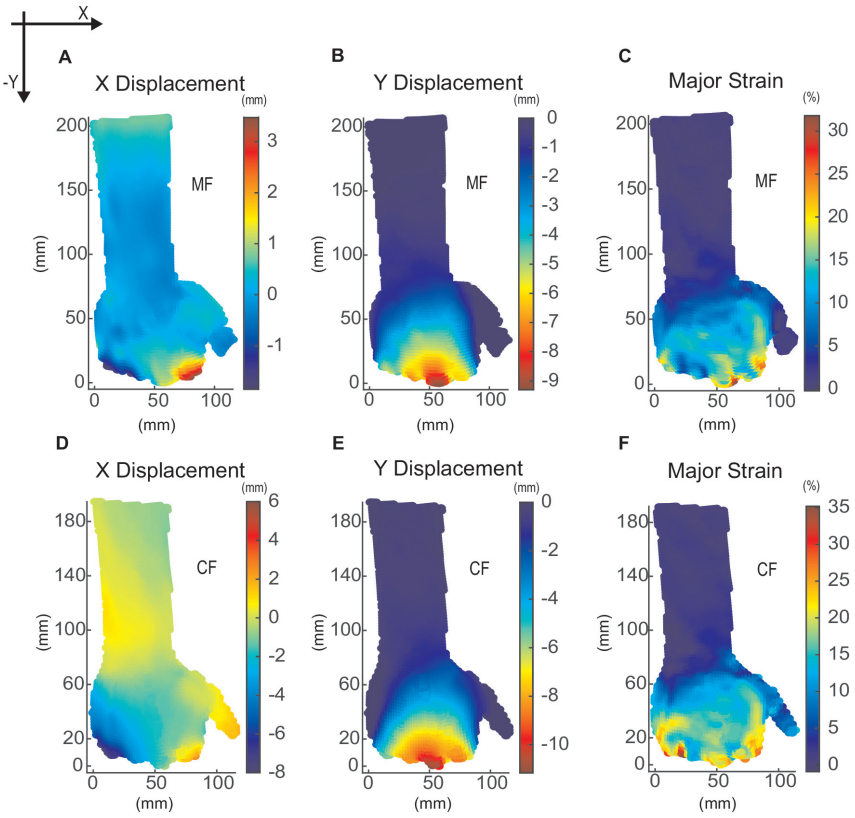

Figure 2. Displacement and major strain fields in dorsal forearm and hand dorsum for metacarpophalangeal flexion and composite fist movements: a) displacement field in the x-axis direction (medial to lateral) caused by metacarpophalangeal flexion MF, b) displacement field in the y- axis direction (proximal to distal) caused by metacarpophalangeal flexion MF, c) Major strain field due to metacarpophalangeal flexion MF, d) displacement field in the x-axis direction caused by composite fist CF, e) displacement field in the y-axis direction caused by composite fist CF, f) Major strain field due to composite fist CF.

https://doi.org/10.22201/fi.25940732e.2025.26.4.025

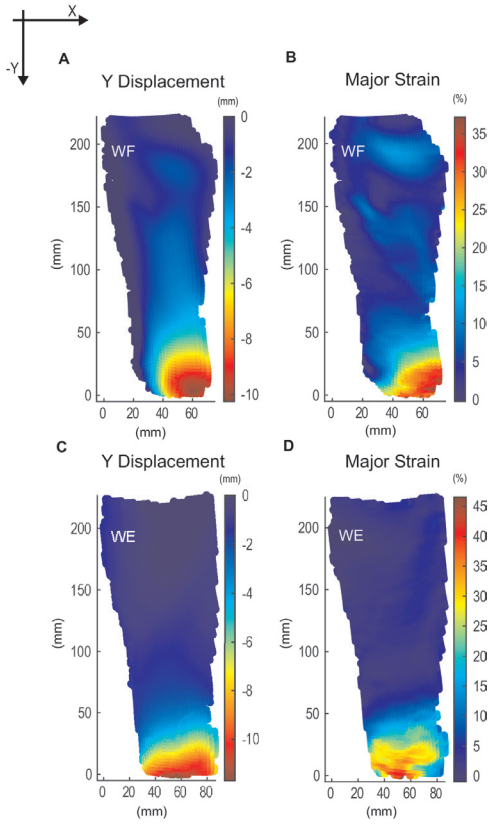

Figure 3. Detailed quantification of displacement along the central line of the displacement and major strain fields for wrist flexion and extension: a) displacement field in the y-axis direction caused by wrist flexion WF (dorsal forearm), b) major strain field caused by wrist flexion WF (dorsal forearm), c) displacement field in the y-axis direction caused by wrist extension WE (volar forearm), d) major strain field caused by wrist extension WE (volar forearm).

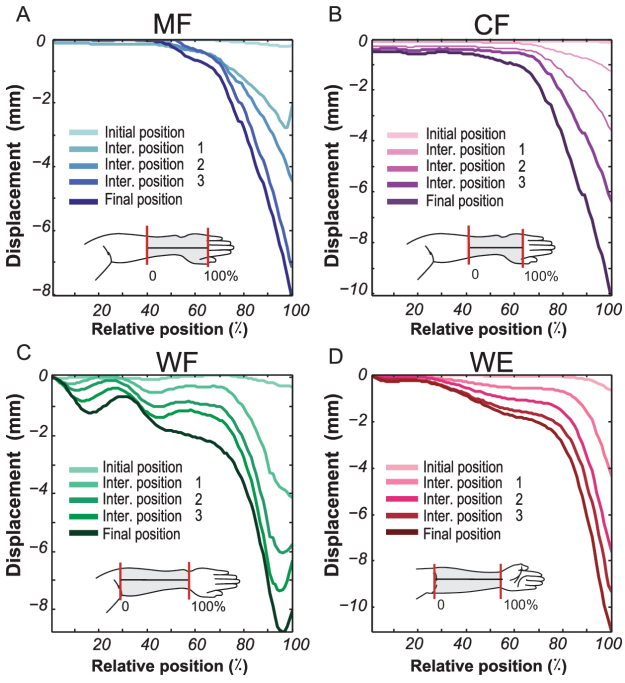

Figure 4. Five sequential positions and their corresponding displacement profiles along the longitudinal axis of the forearm and dorsal hand are shown for: a) metacarpophalangeal flexion, b) composite fist CF, c) wrist flexion WF, d) wrist extension WE. The inserts of the figures depict the region of interest where the measurements were conducted.

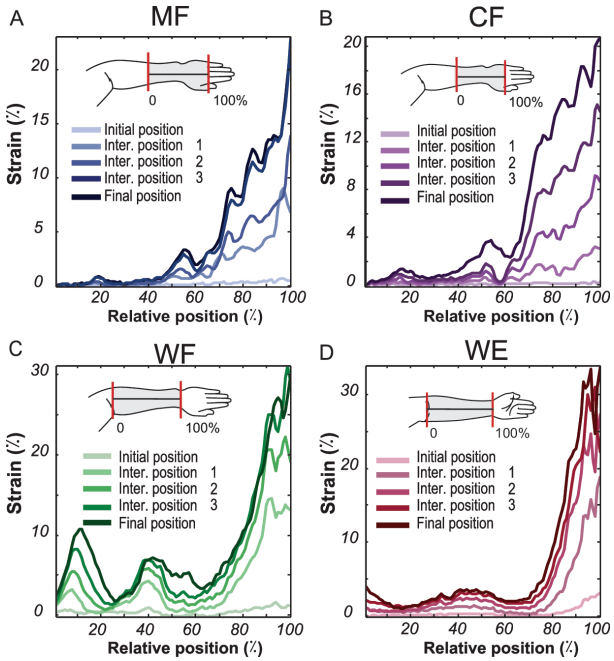

Figure 5. Five sequential positions showing major strain profiles along a central line for the following movements: a) metacarpophalangeal flexion MF, b) composite fist CF, c) wrist flexion WF and d) wrist extension WE.

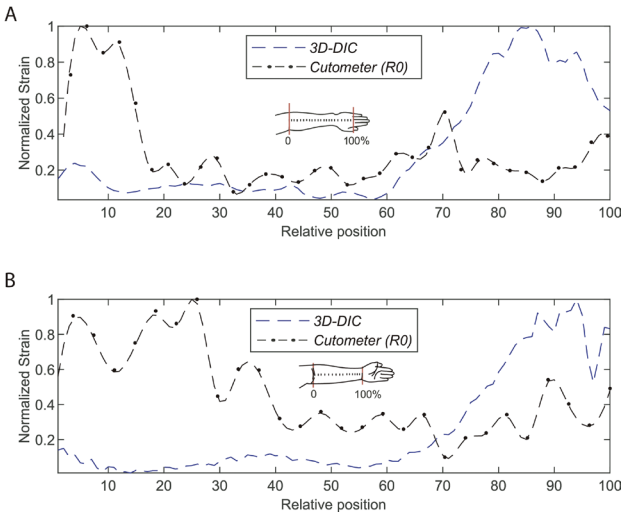

Figure 6. Normalized strain measurements of human skin using 3D-DIC and cutometry, along with a relative position of the forearm: a) dorsal hand and forearm during metacarpophalangeal flexion MF, b) volar forearm as shown in the inset, during wrist extension WE.

Discussion

Joint motion requires coordinated recruitment of the skin surrounding the articulations. During this process, skin must stretch, shift, or contract to accommodate the underlying mechanical demand. In this study, we used 3D-Digital Image Correlation (3D-DIC) to map the dynamic strain and displacement fields of the skin in vivo, across the upper extremity, during full articular motion. This method enabled full-field quantification of skin biomechanics with sub-millimetric resolution, an improvement of several orders of magnitude compared to prior photographic techniques.

Unlike conventional assessment tools used in burn rehabilitation such as the Vancouver Scar Scale or Cutometry, which provide either subjective or localized measures, 3D-DIC offers spatially continuous data independent of the evaluator's experience. Moreover, it captures how skin behaves under functional, physiologically relevant conditions, such as voluntary joint motion, rather than artificial loading (e.g., suction or manual manipulation). This distinction is critical for understanding how scars or grafted skin respond during real-life movement, which ultimately determines function and quality of life.

The displacement and strain maps obtained in this study revealed consistent semicircular patterns surrounding the metacarpophalangeal and radiocarpal joints. These findings suggest the presence of mechanically distinct skin regions-possibly analogous to the "cutaneous functional units" proposed by Richard *et al.* (2009), but now quantified in greater detail. These patterns could inform surgical approaches for contracture release or skin flap design, by identifying where tissue recruitment occurs naturally and how much motion each area supports.

Furthermore, by separating displacement from strain, 3D-DIC allows clinicians and researchers to differentiate between passive tissue translation and active mechanical deformation. This could be particularly useful in monitoring scar evolution, identifying stiffness zones in hypertrophic tissue, or evaluating the effectiveness of new bioengineered skin substitutes. In clinical practice, such insights may support decision-making on when to initiate or adjust therapy, how to plan surgical interventions, or how to objectively measure treatment outcomes over time.

This study employed an exploratory design with healthy participants to establish the feasibility and reproducibility of 3D-DIC in mapping skin deformation during common joint gestures. These movements, metacarpophalangeal flexion, composite fist, wrist flexion, and wrist extension, were selected due to their clinical relevance, as they are routinely evaluated in post-burn assessments. Yet, no prior literature has quantified where the skin moves from, or how it deforms, to enable these gestures. Our findings begin to fill this gap and provide a reference for future comparisons.

Limitations

This study has several limitations. First, the small and homogeneous sample (n = 3, healthy young males) limits the generalizability of the results. Second, no pathological or scarred skin was included, so clinical applicability remains to be validated in patient populations. Third, although motion was standardized, we did not test variations in movement speed or loading, which could influence strain responses. Future research should incorporate diverse subjects, including individuals with post-burn scarring or skin grafts, to establish the diagnostic and prognostic value of 3D-DIC in real-world clinical contexts.

Conclusions

This study demonstrated that 3D-Digital Image Correlation (3D-DIC) is a valuable technique for quantifying full-field skin strain and displacement in the upper extremity during the complete articular range of motion. The method revealed reproducible semicircular recruitment patterns, previously undescribed, that support a biomechanical basis for skin movement across functional units of the hand and forearm. The technique provided sub-millimetric resolution, improving upon previous photographic approaches by several orders of magnitude, and enabling detailed analysis of tissue mechanics that are directly relevant to clinical decision-making.

Beyond its technical precision, 3D-DIC offers concrete clinical potential. In burn management, accurate assessment of skin extensibility and deformation is essential to guide therapeutic strategies. The ability to visualize and quantify how much, and from where, skin is recruited to permit movement could inform the surgical planning of contracture releases, the design and evaluation of skin grafts or engineered tissue constructs, and the optimization of physical therapy regimens to target specific areas of functional limitation. Moreover, the technique could assist in the objective monitoring of scar progression over time or under different treatment protocols.

As such, 3D-DIC represents not only methodological advancement but a promising clinical tool for reconstructive and rehabilitative strategies in patients with burns and other conditions involving skin mobility impairments. Future studies involving clinical populations will be necessary to validate its utility in real-world therapeutic contexts and to establish normative data across age groups, body types, and pathological states.

Acknowledgments

Funding Information: Álvarez-Camacho, Michelín, Conacyt Salud. Grant Number 2010/141036. Aguilar-Ordaz, Karen-Edith and Cruz-Chavarría Ximena as editors.

References

Agache, P. G., Monneur, C., Leveque, J. L., & De Rigal, J. (1980). Mechanical properties and Young's modulus of human skin in vivo. *Archives of Dermatological Research*, 269(3), 221-232. https://doi.org/10.1007/bf00406415

Barel, A. O., Lambrecht, R., & Clarys, P. (1998). Mechanical function of the skin: state of the art. *Curr Probl Dermatol*. (26), 69-83. https://doi.org/10.1159/000060577

Blair, M. J., Jones, J. D., Woessner, A. E., & Quinn, K. P. (2020). Skin structure-function relationships and the wound healing

response to intrinsic aging. *Advances in wound care*, 9(3), 127-143. https://doi.org/10.1089/wound.2019.1021

Boyer, G., Pailer-Mattei, C., Molimard, J., Pericoi, M., Laquieze, S., & Zahouani, H. (2011). Non contact method for in vivo assessment of skin mechanical properties for assessing effect of ageing. *Medical Engineering & Physics*, 34(2), 172 8. https://doi.org/10.1016/j.medengphy.2011.07.007

Cai, L., Lippi, J., Dumanian, J., Klein, M., Dangol, M. K., Puri, V., … Chang, J. (2017). Development of international outcomes instrument for hand and upper extremity burn scar contracture release. *Journal of Burn Care & Research*, 38(1), e395-e401. https://doi.org/10.1097/BCR.0000000000000403

Chen, B., Genovese, K., & Pan, B. (2020). In vivo panoramic human skin shape and deformation measurement using mirror-assisted multi-view digital image correlation. *Journal of the Mechanical Behavior of Biomedical Material*, 110. https://doi.org/10.1016/j.jmbbm.2020.103936

Delalleau, A., Josse, G., Lagarde, J. M., Zahouani, H., & Bergheau, J. M. (2008). Characterization of the mechanical properties of skin by inverse analysis combined with an extensometry test. *Waer*, 264(5-6), 405-410. https://doi.org/10.1016/j.wear.2006.08.033

Diridollou, S., Patat, F., Gens, F., Vaillant, L., Black, D., Lagarde, J. M., … Berson, M. (2000). In vivo model of the mechanical properties of the human skin under suction. *Skin Research and Technology*, 6(4), 214-221. https://doi.org/10.1034/j.1600-0846.2000.006004214.x

Draaijers, J., Tempelman, R., Botman, Y., Tuinebreijer, E., Middelkoop, E., Kreis, R., & van Zuijlen, P. (2004). The patient and observer scar assessment scale: A reliable and feasible tool for scar evaluation. *Plastic and Recontructive Surgery*, 113(7), 1960-1965. https://doi.org/10.1097/01.prs.0000122207.28773.56

Elseth, A., & Nunez-Lopez, O. (2021). *Wound grafts.* StatPearls Publishing.

Evans, S. L., & Holt, C. A. (2009). Measuring the mechanical properties of human skin in vivo using digital image correlation and finite element modelling. *The Journal of Strain Analysis for Engineering Design*, 44(5), 337-345. https://doi.org/10.1243/03093247JSA488

Fearmonti, R., Bond, J., Erdmann, D., & Levinson, H. (2010). A review of scar scales and scar measuring devices. *EPlasty*, 43(10).

Frykberg, R. G., & Banks, J. (2015). Challenges in the treatment of chronic wounds. *Advances in Wound Care*, 4(9), 560-582. https://doi.org/10.1089/wound.2015.0635

Held, M., Rahmanian-Schwarz, A., Rothenberger, J., Schiefer, J., Janghorban Esfahani, B., Schaller, H. E., & Jaminet, P. (2014). Alteration of biomechanical properties of burned skin. *Burns*, 41(4), 789-95. https://doi.org/10.1016/j.burns.2014.09.021

Järbrink, K., Ni, G., Sönnergren, H., Schmidtchen, A., Pang, C., Bajpai, R., & Car, J. (2016). Prevalence and incidence of chronic wounds and related complications: A protocol for a systematic review. *Sysrtematic Reviews*, 5(1). https://doi.org/10.1186/s13643-016-0329-y

Khatam, H., Reece, G. P., Fingeret, M. C., Markey, M. K., & Ravi-Chandar, K. (2014). In-vivo quantification of human breast deformation associated with the position change from supine to upright. *Medical Engineering & Physics*, 37(1), 13-22. https://doi.org/10.1016/j.medengphy.2014.09.016

Maiti, R., Gerhardt, L.-C., Lee, Z. S., & Byers, R. A. (2016). In vivo measurement of skin surface strain and sub-surface layer deformation induced by natural tissue stretching. *Journal of the Mechanical Behavior of Biomedical Material*, 62, 556-569. https://doi.org/10.1016/j.jmbbm.2016.05.035

Marcellier, H., Vescovo, P., Varchon, D., Vacher, P., & Humbert, P. (2001). Optical analysis of displacement and strain fields on human skin. *Skin Research and Technology*, 7(4), 246-53. https://doi.org/10.1034/j.1600-0846.2001.70407.x

Maslauskas, K., Rimdeika, R., Rapoliene, J., Saladzinskas, Z., Samsanavicius, D., & Kaikaris, V. (2009). The comparison of two methods of treatment evaluating complications and deficiency of functions of hands after deep partial skin thickness hand burns. *Medicina*, 45(1), 37-45.

Moore, M., Dewey, W., & Richard, R. (2009). Rehabilitation of the burned hand. *Hand Clinics*, 25(4). https://doi.org/10.1016/j.hcl.2009.06.005

Mueller, B., Elrod, J., Distler, O., Schiestl, C., & Mazza, E. (2021). On the reliability of suction measurements for skin characterization. *Journal of Biomedical Engineering*, 143(2). https://doi.org/10.1115/1.4047661

Nedelec, B., Shankowsky, H. A., & Tredget, E. E. (2000). Rating the resolving hypertrophic scar. *Journal of Burn Care & Rehabilitation*, 21(3), 205-212. https://doi.org/10.1097/00004630-200021030-00005

Olsson, M., Järbrink, K., Divakar, U., Bajpai, R., Upton, Z., Schmidtchen, A., & Car, J. (2018). The humanistic and economic burden of chronic wounds: A systematic review. *Wound Repair and Regeneration*, 27(1), 114-125. https://doi.org/10.1111/wrr.12683

Pailler-Mattei, C., Bec, S., & Zahouani, H. (2008). In vivo measurements of the elastic mechanical properties of human skin by indentation tests. *Medical Engineering & Physics*, 30(5), 599-606. https://doi.org/10.1016/j.medengphy.2007.06.011

Podwojewski, F., Otténio, M., Beillas, P., Guérin, G., Turquier, F., & Mitton, D. (2014). Mechanical response of human abdominal walls ex vivo: Effect of an incisional hernia and a mesh repair. *Journal of the Mechanical Behavior of Biomedical Material*, 38, 126-33. https://doi.org/10.1016/j.jmbbm.2014.07.002

Richard, R. L., Lester, M. E., Miller, S. F., Bailey, J. K., Hedman, T. L., Dewey, W. S., Blackbourne, L. H. (2009). Identification of cutaneous functional units related to burn scar contracture development. *Journal of Burn Care & Research*, 30(4), 625-631. https://doi.org/10.1097/BCR.0b013e3181ac016c

Solav, D., Moerman, K. M., Jaeger, A. M., Genovese, K., Herr, H. M. (2018). MultiDIC: An open-source toolbox for multi-view 3D digital image correlation. In IEEE Access, 6, 30520-30535. https://doi.org/10.1109/ACCESS.2018.2843725

Sullivan, T., Smith, J., Kermode, J., Mclver, E., & Courtemanche, D. J. (1990). Rating the burn scar. *Journal of Burn Care & Rehabilitation*, 11(3), 256-260. https://doi.org/10.1097/00004630-199005000-00014

Ud-Din, S., & Bayat, A. (2016). Non-invasive objective devices for monitoring the inflammatory, proliferative and remodelling phases of cutaneous wound healing and skin scarring. *Experimental Dermatology*, 25(8),579-585. https://doi.org/10.1111/exd.13027

Van-Alphen, T. C., Ter-Brugge, F., van-Haren, E. L., Hoogbergen, M. M., & Rakhorst, H. (2023). SCI-QOL and WOUND-Q have the best patient-reported outcome measure design: A systematic literature review of PROMs used in chronic wounds. *Plastic and Reconstructive Surgery-Global Open*, 11(1), e4723. https://doi.org/10.1097/GOX.0000000000004723

Vázquez, N., Sánchez-Arévalo, F., Maciel-Cerda, A., Garnica-Palafox, I., Ontiveros-Tlachi, R., & Chaires-Rosas, C. (2019). Influence of the PLGA/gelatin ratio on the physical, chemical and biological properties of electrospun scaffolds for wound dressings. *Biomedical Materials*, 14(4), 256-260. https://doi.org/10.1088/1748-605x/ab1741

Wilson, A. J., Chin, B. C., Hsu, V. M., Mirzabeigi, M. N., & Percec, I. (2015). Digital image correlation: A novel dynamic three-dimensional imaging technique for precise quantification of the dynamic rhytid and botulinum toxin type a efficacy. *Plastic and Recontructive Surgery*, 135(5), 869-876. https://doi.org/10.1097/prs.0000000000001224

Xu, Z., Dela-Cruz, J., Fthenakis, C., & Saliou, C. (2019). A novel method to measure skin mechanical properties with three-dimensional digital image correlation. *Skin Research and Technology*, 25(1), 60-67. https://doi.org/10.1111/srt.12596

Xue, Y., Cheng, T., Xu, X., Gao, Z., & Li, Q. *et al.* (2017). High-accuracy and real-time 3D positioning, tracking system for medical imaging applications based on 3D digital image correlation. *Optics and Lasers in Engineering*, 88, 82-90. https://doi.org/10.1016/j.optlaseng.2016.07.002

Zheng, Y. P., Choi, Y. K., Wong, K., Chan, S., & Mak, A. F. (2000). Biomechanical assessment of plantar foot tissue in diabetic patients using an ultrasound indentation system. *Ultrasound in Medicine and Biology*, 26(3), 451-456. https://doi.org/10.1016/S0301-5629(99)00163-5

How to cite:

López-Lugo, J. D., Benítez-Martínez, J. A., Alvarez-Camacho, M., Leyva-Gómez, G., Morales-García, M., Palacios-Morales, C., & Sánchez-Arévalo, F. M. (2025). Quantitative and objective full-field strain measurements of healthy human skin during distal upper extremity range of motion. *Ingeniería Investigación y Tecnología,* 26(04), 1-12. https://doi.org/10.22201/fi.25940732e.2025.26.4.025